Growth Process of ZSM-5 Zeolite Film

Tsuneji SANO,* Fujio MIZUKAMI, Haruo TAKAYA, Takashi MOURI,† and Masami WATANABE††
National Chemical Laboratory for Industry, Tsukuba, Ibaraki 305
† Tosoh Co., Ltd., Shinnanyo, Yamaguchi 746
†† Ishikawajima-Harima Heavy Industries Co., Ltd., Koto-ku, Tokyo 135
(Received Agust 1, 1991)

The growth process of a ZSM-5 zeolite film was studied using EDX-SEM, TEM, and EDX-STEM. It became clear that the ZSM-5 zeolite film was formed through a successive accumulation of zeolite crystals of 5 to 10 μm size. It was also found that the crystalline embryos with high Al concentration existed in the vicinity of the inner side of the zeolite film and within the film.

Great interest has been focused on membrane separation technology. Various types of organic and inorganic membranes have been developed. Recently, the preparation of zeolite films or membranes has also been studied, due to their pore sizes and resistance to high temperatures.[1)]

More recently, we have found that the ZSM-5 zeolite films 30—100 μm thickness, which are made up of zeolite crystals themselves, can be prepared from a clear aqueous solution of a synthesis mixture with a high H_2O/SiO_2 ratio.[2)] Large differences in the surface morphology and the surface SiO_2/Al_2O_3 ratio between both sides of the films were observed. In order to obtain a better understanding of the zeolite film, the growth process of the film was studied in detail. Scanning electron microscopy (morphology), transmission electron microscopy (morphology and micro-crystallization), and scanning transmission electron microscopy (analysis by X-ray emission spectrometry) were employed in the present study.

Experimental

The hydrothermal synthesis of ZSM-5 zeolite films was performed as follows. Aluminum nitrate and colloidal silica (Cataloid SI-30 from Shokubai Kasei Co.; 30.4 wt% SiO_2, 0.38 wt% Na_2O, 69.22 wt% water) were added to a stirred mixture of tetrapropylammonium bromide (TPABr) and sodium hydroxide in solution, to give a hydrogel with a composition of 0.1 TPABr–0.05 Na_2O–0.01 Al_2O_3-SiO_2–80 H_2O. The hydrogel was then transferred to a 50 ml stainless-steel autoclave with a Teflon sleeve. A Teflon slab was immersed in the solution and placed vertically along the axis of the autoclave. The autoclave was placed in an air-heated oven at 443 K for appropriate periods. After the appropriate periods, the autoclave was cooled down, and the slab was then recovered. The zeolite film was removed from the surface of the Teflon slab by mechanical separation, washed with deionized water and dried at 393 K for 24 h. The gel in the solution was also filtered off, washed and dried.

The surface morphology and the surface SiO_2/Al_2O_3 ratio of the zeolite film were measured by scanning electron microscopy (SEM, Hitachi H-800), and an energy-dispersive X-ray analysis (EDX) on a Kevex Delta system attached to the microscope. The bulk SiO_2/Al_2O_3 ratio of the film was determined using an X-ray fluorescence spectroscope (Rigaku 3080E). A complementary characterization was performed using a high-resolution transmission microscope (TEM, Hitachi H-800UHR) and a scanning transmission electron microscope (STEM) with a very high spatial resolution from Vacuum Generators (HB 501). A local chemical analysis (EDX-STEM) was used for the determination of the SiO_2/Al_2O_3 ratio across the cross section of a film with a Si–Li detector linked to a Kevex Super 8000. Ultra-thin sections of the solid were made using an ultra-microtome after the zeolite film was embedded in an epoxy resin.

Results and Discussion

A series of crystallizations of ZSM-5 zeolite films was conducted on Teflon slabs at varying crystallization times. The zeolite films were obtained on the surfaces of the Teflon slab and the Teflon sleeve, and removed from the Teflon surface by mechanical separation. Due to gravity, powdery zeolite crystals were also obtained on the bottom of the Teflon sleeve, i.e., the face at the bottom of the autoclave. After crystallization for 48 h, about 80% of the hydrogel (the synthesis mixture) was converted to the zeolite film. As zeolite synthesis without stirring required a longer crystallization period, compared to a synthesis under stirring, the gel as well as zeolite crystals existed in the solution after crystallization for 6, 14, and 24 h. Both sides of the zeolite films obtained showed the typical X-ray diffraction pattern of ZSM-5 zeolite. Figures 1 and 2 show the scanning electron micrographs of the outer and the inner sides of the film prepared at varying crystallization times, respectively. The outer and inner sides are defined as the sides in contact with the Teflon slab and the solution, respectively. In the case of the outer side of the film, the surface after crystallization for 6 h consisted of a continuous array of loosely packed crystals 5—10 μm in size (Fig. 1-(A)). As shown in Figs. 1-(B), (C), and (D), the surfaces after crystallization for 14, 24, and 48 h comprised densely packed crystals. The shape of crystals became flatter with the crystallization time. On the other hand, in the case of the inner side, the surfaces after crystallization for 6 and 14 h comprised ZSM-5 zeolite crystals, which were similar to those observed on the outer side (Figs. 2-(A) and (B)). However, the surface of the inner side became gradually covered with a

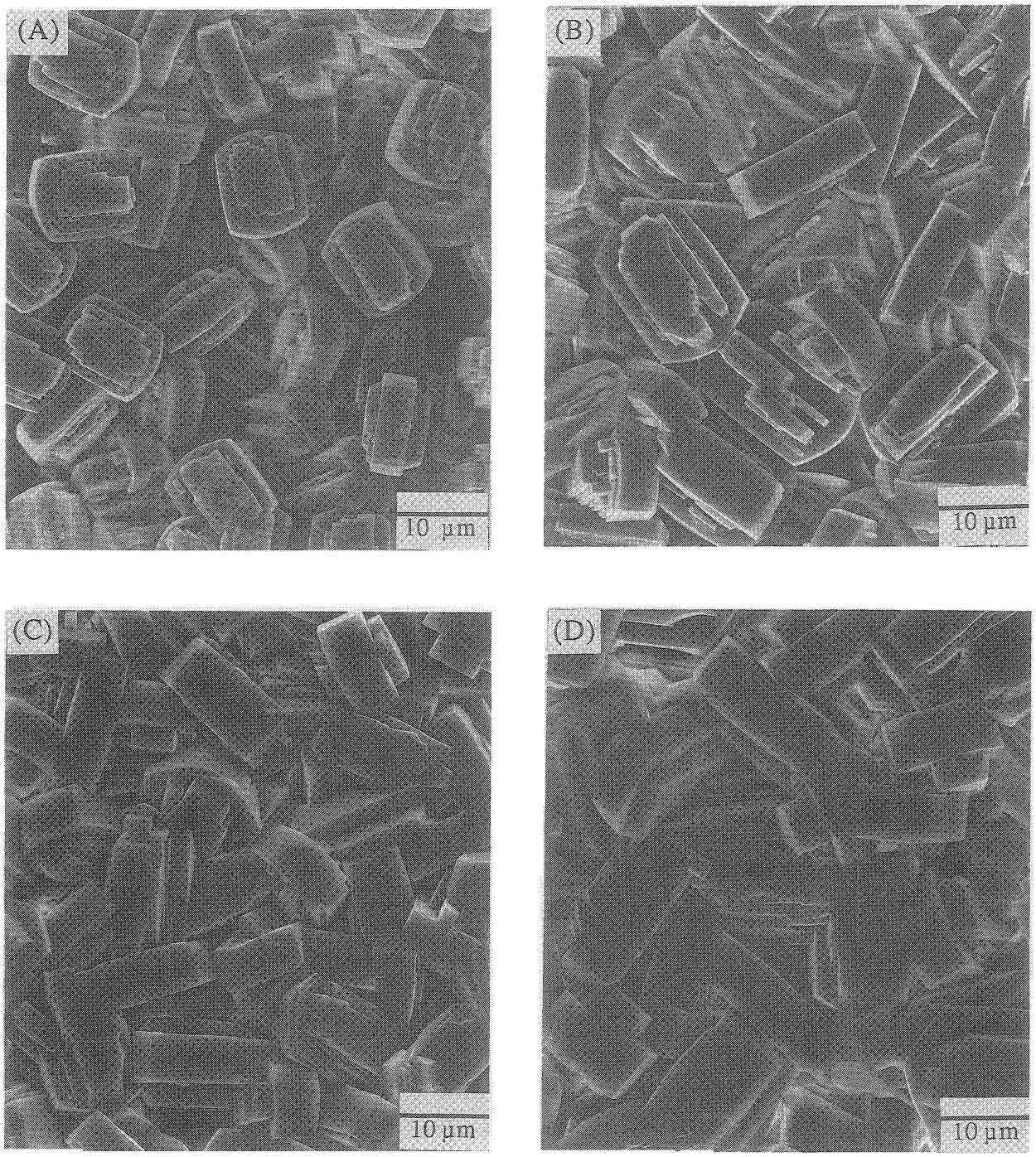

Fig. 1. Scanning electron micrographs of the outer side of zeolite films prepared at varying crystallization times. (A) 6 h, (B) 14 h, (C) 24 h, (D) 48 h.

layer of an aggregate of microcrystals (Fig. 2-(C)), and then the clear shape of the zeolite crystals could not be observed in micrographs after crystallization for 48 h (Fig. 2-(D)). We have already reported that the microcrystals are ZSM-5 zeolites with low crystallinity, and that all Al of the microcrystals are present structurally in the zeolite framework.[2] Auroux et al.[3] as well as Thomas et al.[4] have also described the coexistence of crystalline embryo tiny particles within zeolite grains. These results indicate that the ZSM-5 zeolite film is formed through a successive accumulation of zeolite crystals.

The surface SiO_2/Al_2O_3 ratios of both sides of the films and the thickness of the films are summarized in Table 1. The SiO_2/Al_2O_3 ratios of amorphous materials, the gel in the solution, are also listed. For each sample, 2 or 3

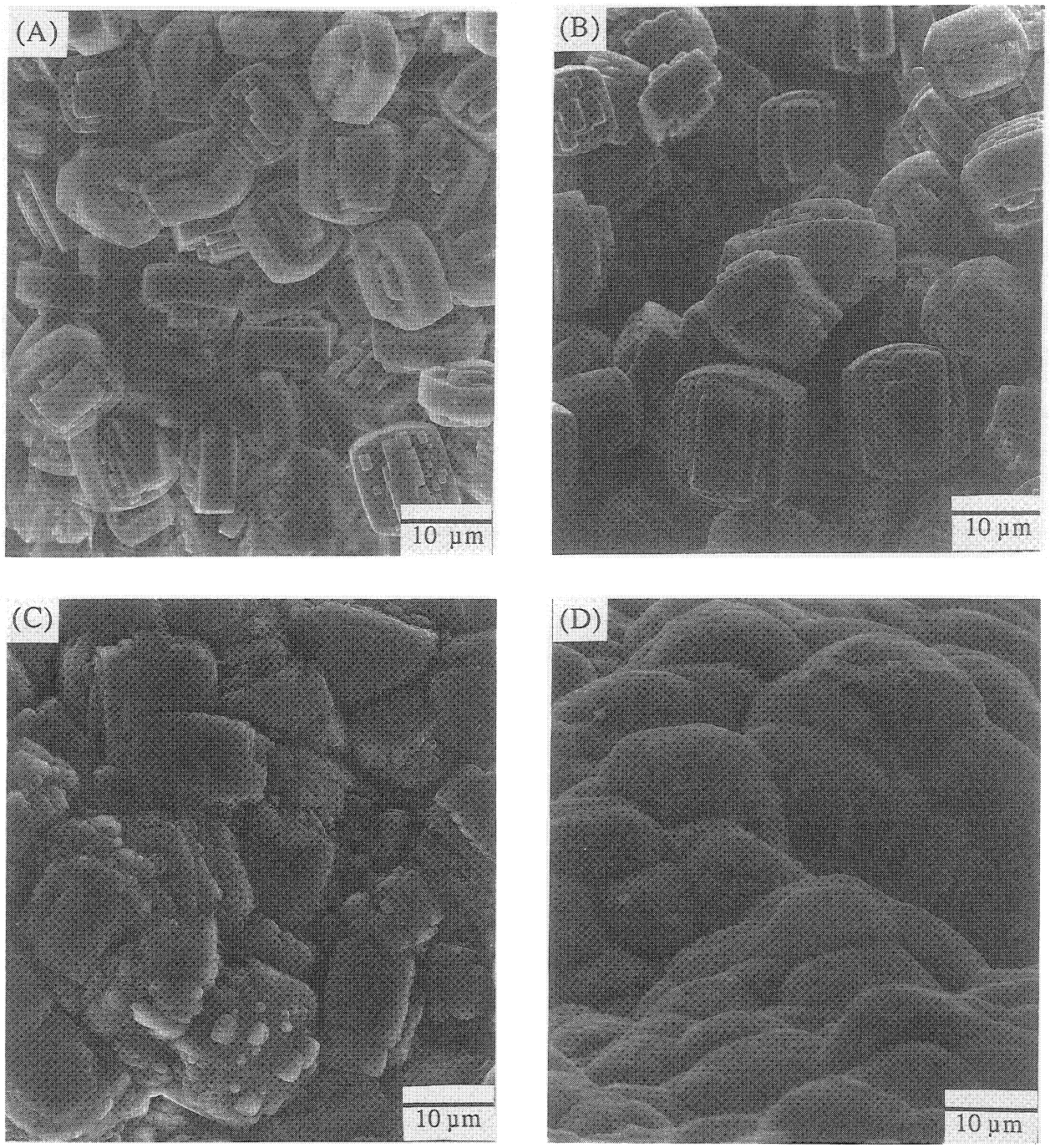

Fig. 2. Scanning electron micrographs of the inner side of zeolite films prepared at varying crystallization times.
(A) 6 h, (B) 14 h, (C) 24 h, (D) 48 h.

analytical points at least were selected in order to accurately evaluate the Al distribution on the surface. Although the values of the SiO_2/Al_2O_3 ratios obtained showed some scatter, there was a definite tendency. The SiO_2/Al_2O_3 ratios of the outer side were much higher than that expected from the composition of the synthesis mixture ($SiO_2/Al_2O_3=100$), and appeared to increase with the crystallization time. On the other hand, the surface SiO_2/Al_2O_3 ratios of the inner side were lower than that of the synthesis mixture and decreased with the crystallization time, indicating an enrichment of Al on the microcrystals. A heterogeneous distribution of Al within a zeolite grain is well recognized.[5] A similar trend regarding the decrease in the SiO_2/Al_2O_3 ratio with the crystallization time was observed for amorphous materials. The bulk SiO_2/Al_2O_3 ratio of the film after

Table 1. Surface SiO_2/Al_2O_3 Ratios and Thickness of Zeolite Films Prepared at Varying Crystallization Times

Time	Thickness	SiO_2/Al_2O_3 ratio determined by EDX		
		Film		
h	μm	Outer[a]	Inner[b]	Amorphous[c]
3	—	—	—	101
				98
				136
6	20—50	189	103	80
		302	158	76
		242	103	
14	20—60	331	72	73
		183	70	65
		231	83	
24	30—80	354	35	67
		234	33	81
		401	76	53
48	30—100	>600[d]	26	
		390	41	
			21	

a) Side in contact with the Teflon slab. b) Side in contact with the solution. c) Confirmed by XRD. d) The content of Al was far below the detection limit of the spectrometer.

48 h of crystallization was 109, which was consistent with the SiO_2/Al_2O_3 ratio of the synthesis mixture. The thickness of the film increased with the crystallization time.

In order to further clarify the properties of zeolite film, the Al distribution and crystallinity across the cross section of the film were monitored by high-resolution TEM and EDX-STEM. Figure 3 shows transmission electron micrographs of the cross section of the film after crystallization for 48 h. As shown in Figs. 3-(A), (B), and (C), the coexistence of (a) a thin layer of about 3000 Å, (b) a well-crystallized region, (c) aggregates of tiny particles, and (d) a grain boundary was pointed out in the vicinity of the inner side. Aggregates of tiny particles and the grain boundary were not observed in the vicinity of the outer side (Fig. 3-(D)). In order to clarify the local crystallinities of these regions, the electron diffractions were measured (Fig. 4). The net pattern was observed for the electron diffraction of (b), shown in Fig. 4-(B). This demonstrates that the region of (b) is well-crystallized. On the other hand, both (a) and (c) did not show systematic diffraction patterns, indicating the existence of crystalline embryos (Figs. 4-(A) and (C)). The electron diffraction pattern of (d) was similar to that of (c). Most regions in the vicinity of the outer side exhibited the net patterns. However, there were a few regions, such as (e) in Fig. 3-(D), which did not show systematic diffraction patterns (Fig. 4-(D)). From the facts that no diffraction peaks, other than ZSM-5 zeolite, were observed in the X-ray diffraction diagram of the outer side, and that the clear shape of the zeolite crystals was observed in the outer side, the local transformation of ZSM-5 zeolite or the coexistence of a crystal with low crystallinity is suggested. However, an assignment could not be made due to the limited data.

The *d*-spacing values for 4—6 diffraction spots in the electron diffraction patterns in Fig. 4 were calculated and compared with the powder X-ray diffraction data of ZSM-5 zeolite reported in the literature[6] (Table 2). For the net pattern in Fig. 4-(B), the indices (*h k l*) of the diffraction spots could be routinely obtained. However, since it was difficult to accurately assign the indices (*h k l*) of the diffraction spots in Figs. 4-(A), (C), and (D), the *d*-spacing values, as close as possible to the calculated values, were selected from the X-ray diffraction data. The calculated *d*-spacing values are in fair agreement with the X-ray diffraction data. It was confirmed that the zeolite film obtained consisted of ZSM-5 type zeolite crystals.

Next, local analyses (ϕ=ca. 200 Å) of the Al and Si concentration across the cross section of the film after crystallization for 48 h were conducted by means of EDX-STEM. Figure 5 shows the change in the SiO_2/Al_2O_3 ratio. The SiO_2/Al_2O_3 ratio gradually increased from the inner to the outer sides. The SiO_2/Al_2O_3 ratio in the vicinity of the outer side was about 320 and, substantially, agreed with the analytical data by EDX-SEM in Table 1. EDX-STEM studies also showed the existence of high Al concentration regions, pointed out by two arrows in Fig. 5, in the cross section of the film. The morphology of the regions with high Al concentration was similar to that of the aggregates of microcrystals shown in Fig. 3-(C), indicating the

Table 2. *d*-Spacing Calculated from Electron Diffraction Pattern

No.	*d*-Spacing (Å)							
	(a)[a]		(b)[a]		(c)[a]		(e)[a]	
	Obsd	Ref.[b]	Obsd	Ref.[b]	Obsd	Ref.[b]	Obsd	Ref.[b]
1	9.93	(9.939:d_{200})	11.18	(11.033:d_{101})	11.15	(11.132:d_{011})	3.91	(3.851:d_{051})
2	7.93	(8.035:d_{021})	11.19	(11.153:$d_{\bar{1}01}$)	9.93	(9.939:d_{200})	3.75	(3.756:$d_{\bar{5}11}$)
3	3.79	(3.798:d_{501})	6.70	(6.684:d_{002})	9.62	(9.673:d_{111})	3.71	(3.711:d_{033})
4	5.99	(5.991:d_{031})	9.86	(9.939:$d_{\bar{2}00}$)	4.93	(4.969:d_{400})	4.35	(4.350:d_{013})
5	5.32	(5.320:d_{212})	3.99	(4.010:d_{402})	5.46	(5.566:$d_{0\bar{2}\bar{2}}$)		
6	4.59	(4.596:d_{132})	6.02	(5.909:d_{301})				

a) (a), (b), (c), and (e) denote the analytical points for electron diffraction in Fig. 3. b) Reference No. 6.

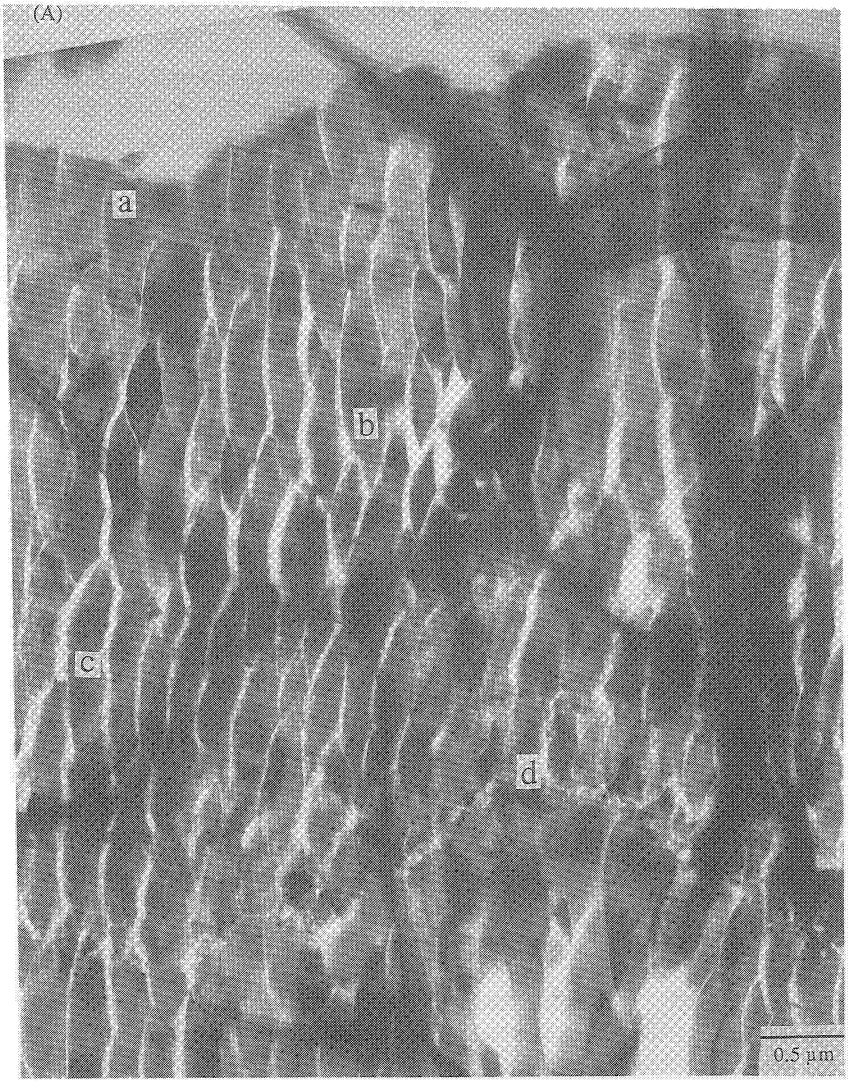
(A)
a
b
c
d
0.5 µm

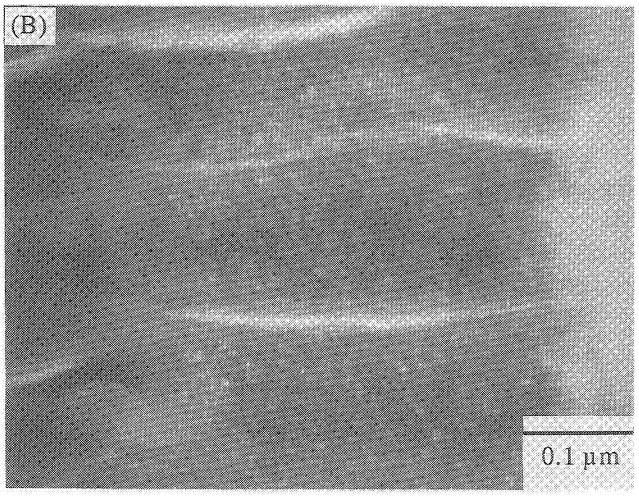
(B)
0.1 µm

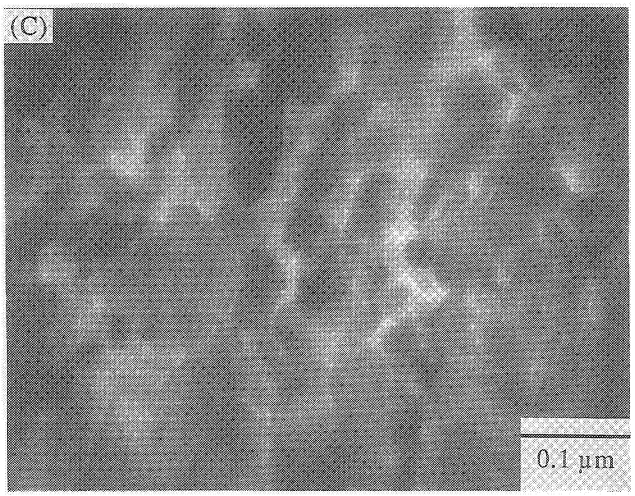
(C)
0.1 µm

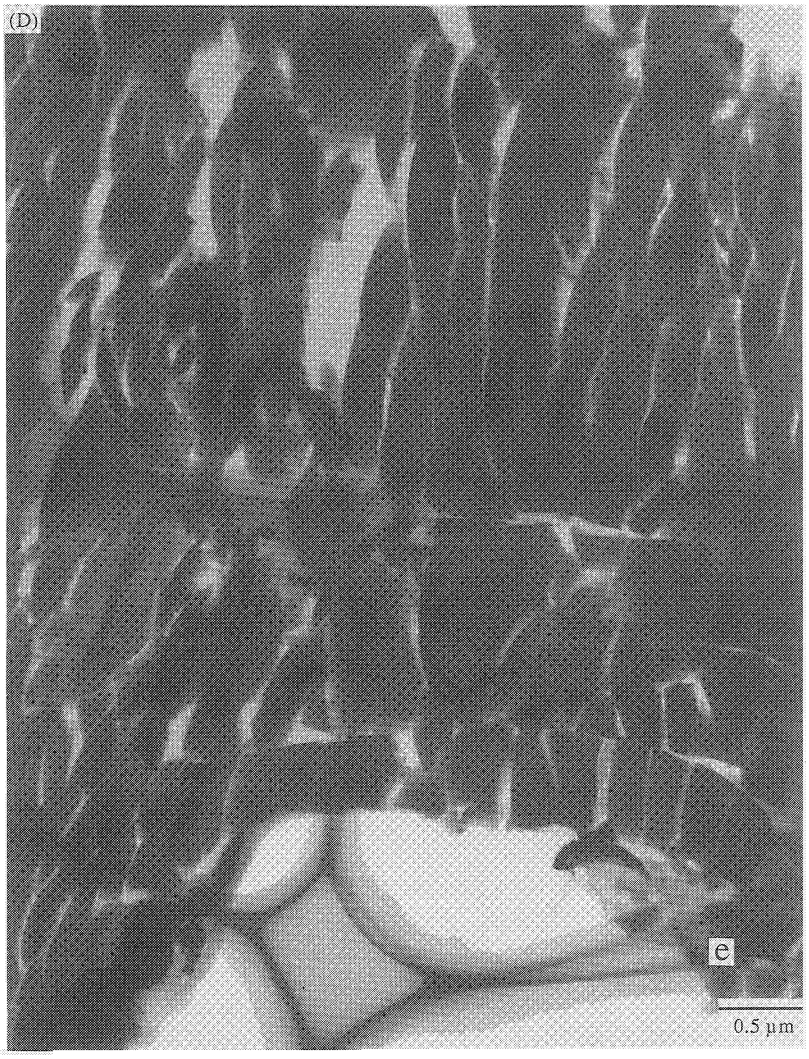

Fig. 3. Transmission electron micrographs of the cross section of zeolite film after crystallization for 48 h. (A) vicinity of the inner side. (B) (a) in (A) at high magnification. (C) (c) in (A) at high magnification. (D) vicinity of the outer side.

coexistence of small quantities of microcrystals with high Al concentration within the film.

As described above, the zeolite film comprises discrete crystals. If the distribution of Al within each zeolite crystal is heterogeneous, the fact that the SiO_2/Al_2O_3 ratio of the cross section of the film gradually increased from the inner to the outer sides is a very puzzling phenomenon. This result therefore seems to suggest that the distribution of Al within each zeolite crystal is relatively homogeneous.

From the above results, it is concluded that the ZSM-5 zeolite film is formed through a successive accumulation of zeolite crystals. Figure 6 shows a diagram of the growth process of the zeolite film. Crystalline embryos with high Al concentration exist in the vicinity of the inner side of the zeolite film and within the film. We generally use Teflon to line zeolite autoclaves for the very reason that since the solution does not wet the Teflon surface, contamination is minimized, nucleation on the walls is minimized, and the deposit of crystals is minimized. An exact interpretation of the role of the Teflon surface in the preparation of the zeolite film can not be given at present due to the limited data.

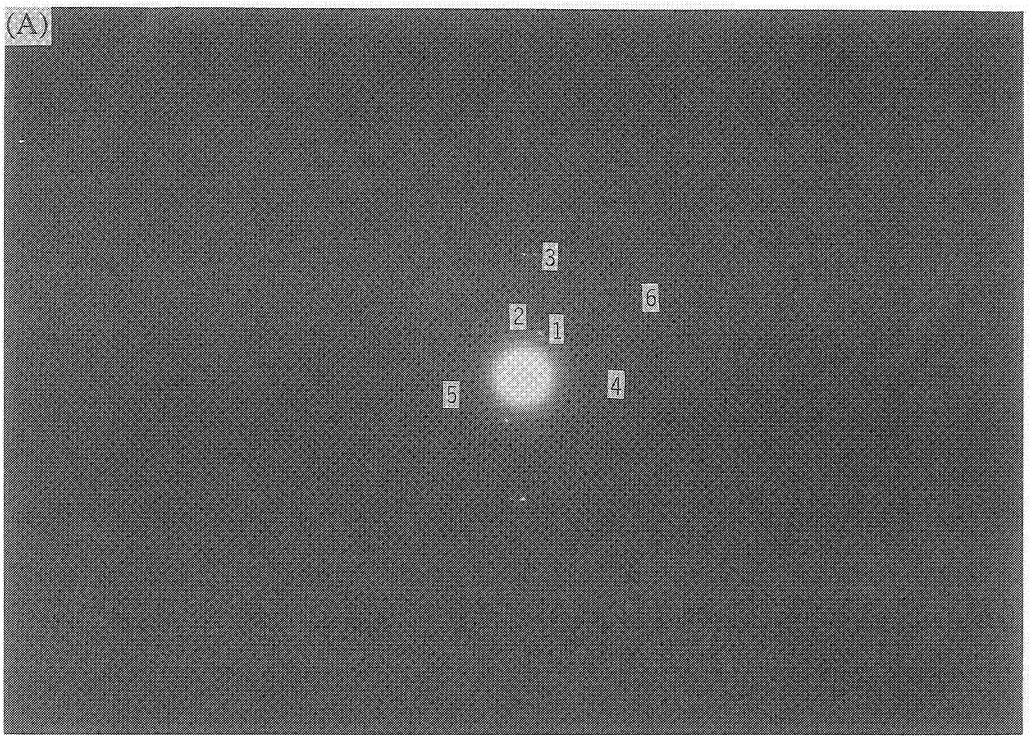
(A)
3
6
2
1
5
4

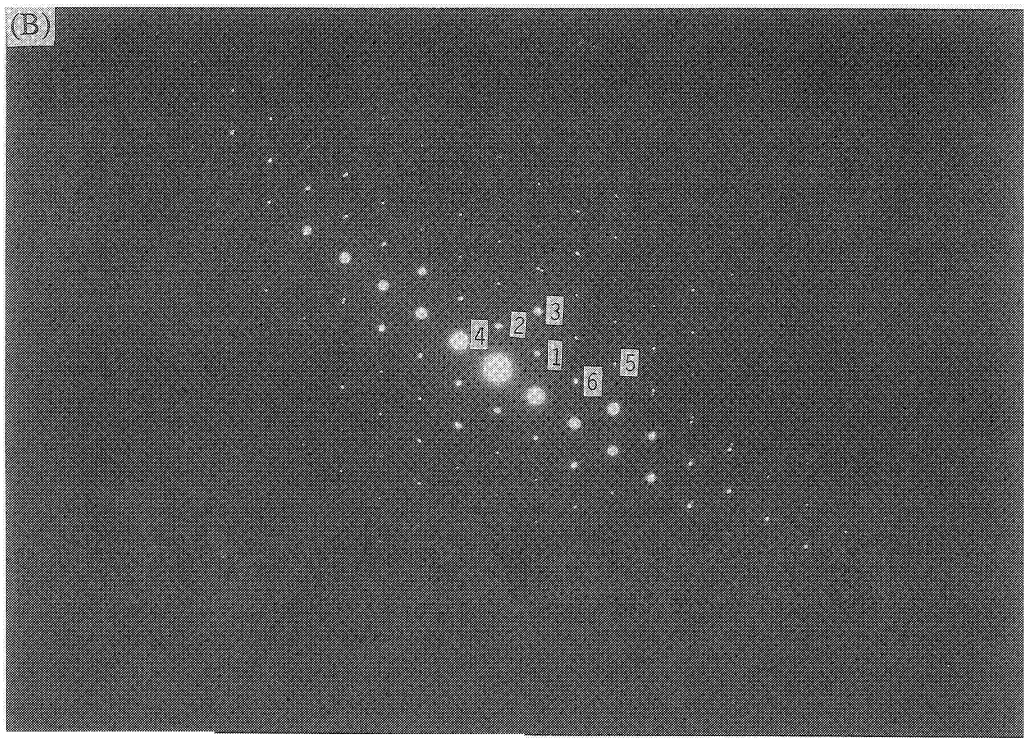
(B)
3
2
4
1
5
6

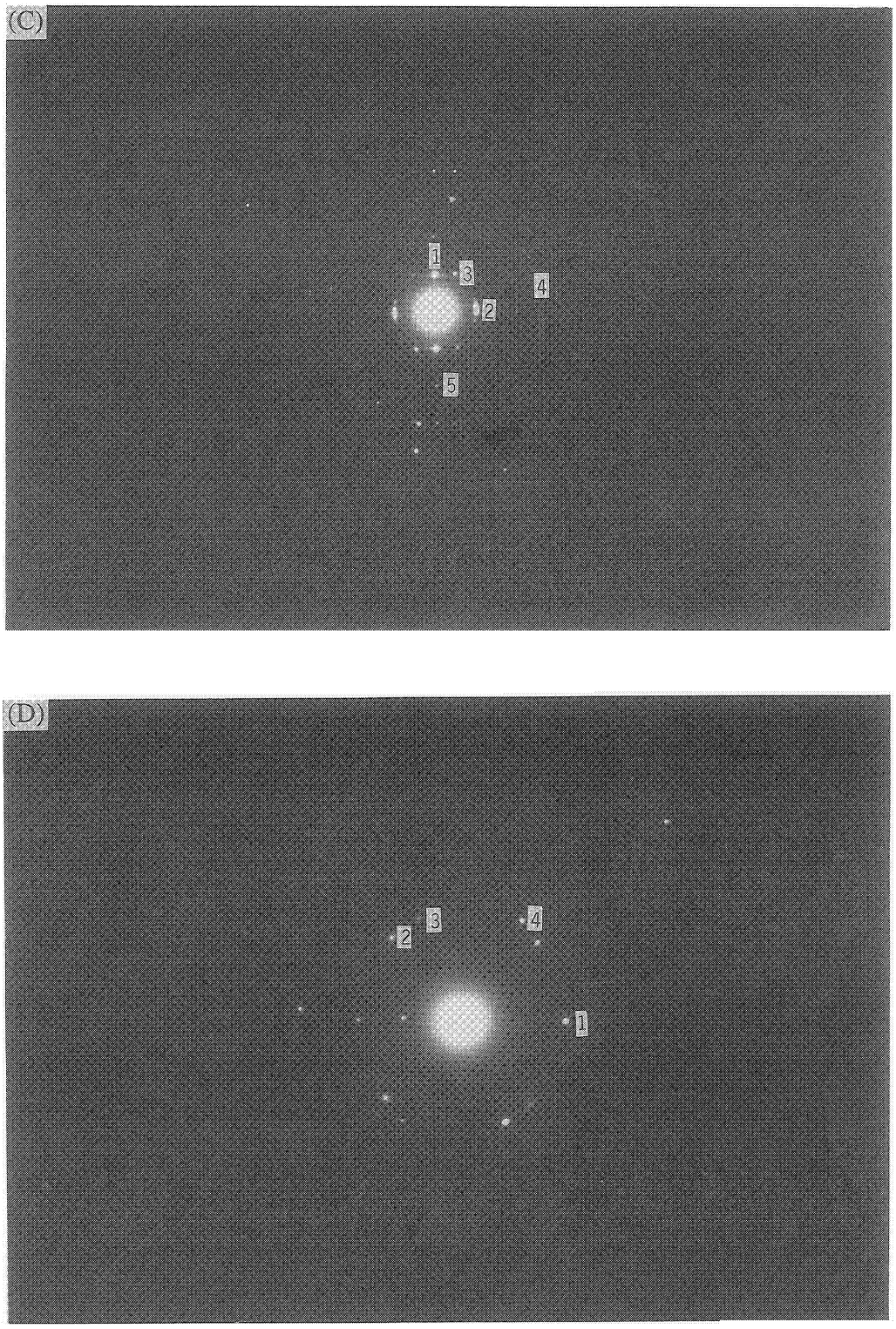

Fig. 4. Electron diffraction patterns of zeolite film. (A) (a) in Fig. 3-(A). (B) (b) in Fig. 3-(A). (C) (c) in Fig. 3-(A). (D) (e) in Fig. 3-(D).

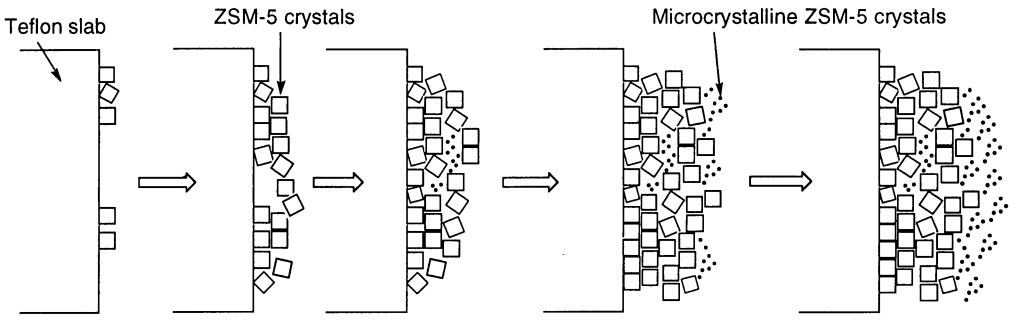

Fig. 6. Schematic growth process of ZSM-5 zeolite film.

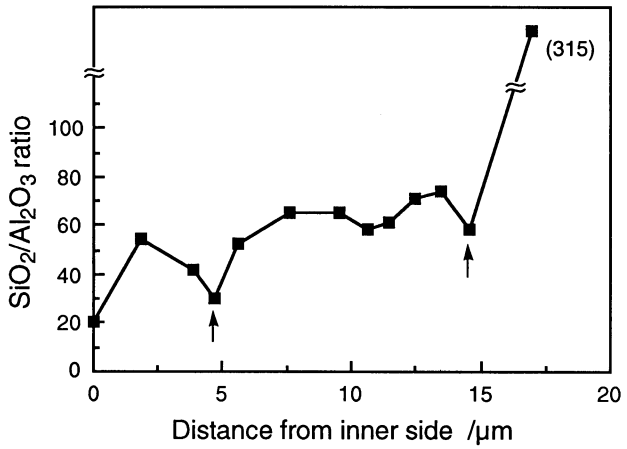

Fig. 5. Local analysis of the SiO_2/Al_2O_3 ratios across the cross section of zeolite film after crystallization for 48 h.

References

1) For example, 1) D. L. Wernick and E. J. Osterhuber, *J. Membr. Sci.*, **22**, 137 (1985). 2) M. Demertzis and N. P. Evmiridis, *J. Chem. Soc., Farady Trans.*, **82**, 3647 (1986). 3) A. Ishikawa, T. H. Chiang, and F. Toda, *J. Chem. Soc., Chem. Commun.*, **1989**, 764. 4) T. Bein, K. Brown, and C. J. Brinker, *Stud. Surf. Sci. Catal.*, **49**, 887 (1989). 5) M. Goldman, D. Fraenkel, and G. Levin, *J. Appl. Polym. Soc.*, **37**, 1791 (1989). 6) A. S. Michaels, *CHEMTECH*, March **1989**, 162. 7) Jpn. Kokai Tokkyo Koho, 59-213615 (1984). 8) Jpn. Kokai Tokkyo Koho, 63-291809 (1988). 9) US Patent 4800187 (1989).

2) T. Sano, Y. Kiyozumi, M. Kawamura, F. Mizukami, H. Takaya, T. Mouri, W. Inaoka, Y. Toida, M. Watanabe, and K. Toyoda, *Zeolites,* **11**, 842 (1991).

3) A. Auroux, H. Dexpert, C. Leclercq, and J. Vedrine, *Appl. Catal.*, **6**, 95 (1983).

4) J. M. Thomas, G. R. Millward, S. Ramdas, L. A. Bursell, and M. Audier, *Faraday Discuss. Chem. Soc.*, **72**, 345 (1981).

5) E. G. Derouane, S. Detremmerie, Z. Gabelica, and N. Blom, *Appl. Catal.*, **1**, 201 (1981).

6) R. van Ballmoos and J. B. Higgins, *Zeolites,* **10**, 444S (1990).